Journal of General Virology (2004), **85**, 3787–3796 DOI 10.1099/vir.0.80497-0

Studies on the origin and structure of tubules made by the movement protein of *Cowpea mosaic virus*

J. Pouwels,[1] T. van der Velden,[1] J. Willemse,[1] J. W. Borst,[2] J. van Lent,[3] T. Bisseling[1] and J. Wellink[1]

[1,2]Laboratory of Molecular Biology[1] and MicroSpectroscopy Centre[2], Wageningen University, Dreijenlaan 3, 6703 HA Wageningen, The Netherlands

[3]Laboratory of Virology, Wageningen University, Binnenhaven 11, 6709 PD Wageningen, The Netherlands

Correspondence
J. Wellink
joan.wellink@wur.nl

Received 2 August 2004
Accepted 13 September 2004

Cowpea mosaic virus (CPMV) moves from cell to cell by transporting virus particles via tubules formed through plasmodesmata by the movement protein (MP). On the surface of protoplasts, a fusion between the MP and the green fluorescent protein forms similar tubules and peripheral punctate spots. Here it was shown by time-lapse microscopy that tubules can grow out from a subset of these peripheral punctate spots, which are dynamic structures that seem anchored to the plasma membrane. Fluorescence resonance energy transfer experiments showed that MP subunits interacted within the tubule, where they were virtually immobile, confirming that tubules consist of a highly organized MP multimer. Fluorescence recovery after photobleaching experiments with protoplasts, transiently expressing fluorescent plasma membrane-associated proteins of different sizes, indicated that tubules made by CPMV MP do not interact directly with the surrounding plasma membrane. These experiments indicated an indirect interaction between the tubule and the surrounding plasma membrane, possibly via a host plasma membrane protein.

INTRODUCTION

For successful systemic infection, a plant virus must spread throughout the plant, a process that starts with transport from the initially infected cell to neighbouring uninfected cells (cell-to-cell movement) and is followed by transport through the phloem into roots and young developing leaves (systemic movement). Since plant viruses cannot pass through the rigid cell wall, they have evolved ways of exploiting plasmodesmata, the naturally occurring transport channels present between plant cells (Haywood *et al.*, 2002). Normally, only small molecules are able to pass through plasmodesmata, but plant viruses encode one or more proteins, the so-called movement proteins (MPs), that modify the structure of plasmodesmata in such a way that viral transport is enabled. So far, two basic principles for cell-to-cell movement of plant viruses have been described: tubule-guided movement of virus particles and movement as ribonucleoprotein complexes (Lazarowitz & Beachy, 1999).

Cowpea mosaic virus (CPMV), a positive-stranded, bipartite RNA virus belonging to the family *Comoviridae*, moves from cell to cell by transporting virus particles using tubular structures, which connect the infected cell to the neighbouring uninfected cell (Pouwels *et al.*, 2002a). Immunogold labelling has shown that the CPMV MP is present in these tubular structures (van Lent *et al.*, 1990). On the surface of CPMV-infected protoplasts, similar tubular structures are formed, which protrude up to 20 μm into the culture medium, are tightly surrounded by the plasma membrane and have the same ultrastructure as tubules in plant tissue (van Lent *et al.*, 1991). Remarkably, tubules are also formed on protoplasts transiently expressing MP (Wellink *et al.*, 1993), showing that MP is the only viral protein required for tubule formation. So far, protoplasts have proved extremely useful as a model system for studying targeting and assembly of both wt and mutant MPs (Bertens *et al.*, 2000, 2003; Gopinath *et al.*, 2003; Kasteel *et al.*, 1997; Pouwels *et al.*, 2002b, 2003).

Recently, a CPMV variant encoding a fusion between MP and the N terminus of the green fluorescent protein (MP–GFP) was made, which, similar to non-fused MP, accumulated in the cell wall of infected leaf tissue and formed tubules on protoplasts (Gopinath *et al.*, 2003; Pouwels *et al.*, 2002b). Electron microscopy analysis revealed that these tubules were morphologically indistinguishable from tubules made by non-fused MP, except that GFP, which was fused to the C terminus of MP and thus present inside the tubule (Carvalho *et al.*, 2003), prevented the incorporation of virus particles (Gopinath *et al.*, 2003). MP–GFP also accumulated in peripheral punctate spots in protoplasts

(Gopinath *et al.*, 2003; Pouwels *et al.*, 2002b), similar to what has been observed for non-fused CPMV MP (J. Pouwels, unpublished data) and several other plant viral MPs (Canto & Palukaitis, 1999; Heinlein *et al.*, 1998; Huang *et al.*, 2000; Satoh *et al.*, 2000). The function of these peripheral punctate spots is currently unknown, although it has been speculated that, for tubule-forming MPs, these structures are some sort of nucleation site from which tubule formation is initiated (Huang *et al.*, 2000; Pouwels *et al.*, 2002b).

The aim of the research described in this paper was to gain further insight in the origin and structure of tubules made by CPMV MP. To this end, the protoplast expression system was used as a model system. To study the origin of tubules, time-lapse microscopy was performed on protoplasts expressing MP–GFP. Fluorescence resonance energy transfer (FRET), a very powerful tool for studying protein–protein interactions in living cells (Sekar & Periasamy, 2003), was used to determine whether MP–MP interactions take place within tubules. Furthermore, to investigate the interaction of tubules with the surrounding plasma membrane, the diffusion coefficients of fluorescent plasma membrane-associated proteins were determined in the plasma membrane surrounding tubules using fluorescence recovery after photobleaching (FRAP).

METHODS

Construction of plasmids. For the construction of pMON-MP-CFP, the MP gene was amplified from pMM48 (Wellink *et al.*, 1993) using specific primers introducing an *Nco*I and a *Bgl*II restriction site. This PCR product was digested with *Nco*I and *Bgl*II and ligated into *Nco*I/*Bgl*II-digested pMON-ECFP (kindly provided by Gerard van der Krogt, Laboratory of Molecular Biology, Wageningen University, The Netherlands).

For the construction of pMON-110-YFP-Zm7hvr, the 110 kDa protein coding region was amplified from pTB1G (Eggen *et al.*, 1989), which contains the full CPMV RNA1 sequence under the control of a T7 promoter, using specific primers, thereby introducing a *Cla*I site and an *Nco*I site. This fragment was digested with *Cla*I and *Nco*I and cloned into *Cla*I/*Nco*I-digested pMON-YFP-Zm7hvr, which encodes the yellow fluorescent protein (YFP) fused to the 40 C-terminal amino acids (the hypervariable region) of Rho of plant 7 from *Zea mays* (Zm7hvr) (Vermeer *et al.*, 2004).

Inoculation and analysis of cowpea protoplasts. Protoplasts were isolated from cowpea (*Vigna unguiculata* L. 'California Blackeye') leaves and transfected as described previously (van Bokhoven *et al.*, 1993). For cytoskeleton inhibitor studies, protoplasts were divided into two aliquots: one was left untreated and the other was treated with 20 μM latrunculin B or 10 μM oryzalin. Protoplasts were then incubated at 25 °C under continuous illumination. To stop the movement of protoplasts and most of the tubular structures, protoplasts were embedded in 1·3 % low-melting-point (LMP) agarose at 42 h post-inoculation (p.i.) by mixing 100 μl protoplast solution and 200 μl 2 % LMP agarose in protoplast medium, which was first melted and then allowed to cool down to 37 °C. Lower concentrations of LMP agarose did not prevent the movement of tubules (Mas & Beachy, 1998). For cytoskeleton inhibitor experiments, 20 μM latrunculin B or 10 μM oryzalin was added to the 2 % LMP agarose in protoplast medium just before addition to the protoplasts. For all further analyses (time-lapse microscopy, FRET and FRAP), a Zeiss LSM 510 confocal microscope was used with standard filters to visualize fluorescence.

FRET procedure. FRET is a process in which energy is transferred non-radiatively from a fluorescent donor molecule to a fluorescent acceptor molecule (Sekar & Periasamy, 2003). The efficiency of energy transfer is dependent on the molecular distance at an inverse 6th power, ensuring that FRET will only occur if the donor and acceptor molecule are very close together [typically $<$10–70 Å (1–7 nM)], making FRET a powerful tool for studying protein–protein interactions. As the donor emission spectrum has to overlap the acceptor excitation spectrum, only certain pairs of fluorescent molecules, like the cyan fluorescent protein (CFP) and YFP, both spectral variants of GFP, are suitable for FRET experiments. A result of FRET is quenching of CFP (donor) fluorescence and an increase in YFP (acceptor) fluorescence (sensitized emission), since part of the energy of CFP is transferred to YFP instead of being emitted. This phenomenon can be measured by bleaching YFP, which should result in an increase in CFP fluorescence. This technique, also known as acceptor photobleaching (APB), is a well-established method of determining FRET (Bastiaens & Jovin, 1996; Bastiaens *et al.*, 1996; Karpova *et al.*, 2003; Kenworthy, 2001; Wouters *et al.*, 1998). For the APB experiments, YFP was bleached in a defined region of the cell by scanning five to ten times with a 514 nm argon laser line at 50–70 % laser power. To assess the changes in donor and acceptor fluorescence before and after this bleach, CFP and YFP images were made and the fluorescence intensities of the bleached region were measured in each image using the program LSM image explorer, version 3.2.0.70 (Carl Zeiss). To minimize the photobleaching due to this imaging, a very low laser power was used (approx. 1 %).

FRET spectral imaging microscopy (FRET-SPIM) experiments were performed as described previously (Shah *et al.*, 2002).

FRAP procedure. FRAP is a technique that allows calculation of the diffusion coefficient of a fluorescent molecule from the recovery of fluorescence in a bleached area (Axelrod *et al.*, 1976; Phair & Misteli, 2001; Salmon *et al.*, 1984). Therefore YFP–Zm7hvr and 110–YFP–Zm7hvr (see Results) were bleached both in tubular structures and in non-tubular plasma membrane in the same way as described for the FRET procedure (above). The fluorescence intensity in the bleached area was measured using the program LSM image explorer at two time points before bleaching and then every 0·5–2 s for 30–150 s after bleaching, depending on the construct and condition. Using Slidewrite plus for Windows 5.0 (Advanced Graphics Software), these data were then fitted on to the standard recovery curve for two-dimensional diffusion (Salmon *et al.*, 1984):

$$FN_t = FN_0 + (FN_\infty - FN_0)(1 - e^{-kt}) \quad \text{(equation 1)}$$

where FN_t is the total fluorescence in a given region at any time t after bleaching and k is a constant describing the rate of recovery. From the obtained k value, $T_{½}$, i.e. the time required to attain half of the recoverable fluorescence intensity, can be determined using equation 2 (Salmon *et al.*, 1984):

$$T_{½} = \ln 2/k \quad \text{(equation 2)}.$$

With the aid of $T_{½}$, the diffusion coefficient (D) can be determined using equation 3 (Salmon *et al.*, 1984):

$$D = \omega^2/4T_{½} \quad \text{(equation 3)}.$$

When a circular area is bleached, ω is defined as the radius of

the bleached area. However, in the experiments described here, a rectangular area was bleached and therefore ω was defined as half of the length of the bleached region along the tubule or plasma membrane.

RESULTS

Peripheral punctate spots are dynamic structures that constantly exchange MP subunits and can grow out to become a tubule

To determine the function of peripheral punctate spots, time-lapse microscopy (TLM) (Gerlich & Ellenberg, 2003) was performed on protoplasts infected with a CPMV variant expressing MP–GFP and free MP (CPMV MP–GFP; Pouwels *et al.*, 2002b). A prerequisite for TLM (and for FRET and FRAP, see below) is that the sample is immobile during the course of the measurement. However, the protoplasts and tubules present on the protoplasts were moving fairly extensively in the medium (data not shown). Embedding the protoplasts in 1·3 % LMP agarose immobilized the protoplasts and most of the tubular structures, but, importantly, did not affect the number or length of tubules. Therefore, all experiments described in this paper were performed with agarose-embedded protoplasts. The formation of fluorescent tubules on the embedded CPMV MP–GFP-inoculated protoplasts was followed over time using confocal laser-scanning microscopy (CLSM) (Fig. 1 shows the first 90 min). At $t=0$ (46 h p.i.; 4 h after embedding), MP–GFP had clearly accumulated in peripheral punctate spots of various sizes and in tubules, as observed previously (Gopinath *et al.*, 2003). Since CPMV RNA2 is translated into two overlapping polyproteins due to the presence of two in-frame start codons (Pouwels *et al.*, 2002a), GFP is also fused to the cofactor for RNA2 replication, which causes fluorescence to accumulate in the nucleus as well (Gopinath *et al.*, 2000; Kasteel *et al.*, 1993; Pouwels *et al.*, 2002b). During the course of the experiment, at the site of some, mostly small, peripheral punctate spots, a tubule was formed (Fig. 1, arrows), indicating that some peripheral punctate spots can grow out to become a tubule, supporting their proposed role as nucleation sites for tubule formation (Huang *et al.*, 2000; Pouwels *et al.*, 2002b). Under these conditions, the growth rate of the tubule could be estimated to be at least 3 μm h^{-1}, since a 1·5 μm long tubule grew out in less than 30 min. Most of the peripheral punctate spots, however, did not become a tubule, even after 4 h, which was not surprising since the majority of both embedded and non-embedded protoplasts inoculated with CPMV MP–GFP formed many peripheral punctate spots but very few tubules (data not shown).

Peripheral punctate spots should be able to incorporate MP subunits if they are nucleation sites for tubule formation. Therefore, bleaching experiments were performed in which peripheral punctate spots were bleached and followed over time (data not shown). These experiments showed that recovery of fluorescence had already started 5 min after bleaching and continued for the next 30 min until the amount of fluorescence in the bleached peripheral punctate spots reached pre-bleach levels, showing that the majority of the peripheral punctate spots were dynamic structures that were able to incorporate new MP subunits. These data, together with the observation that the majority of peripheral punctate spots did not increase in size, even after 90 min (Fig. 1), indicated that exchange of MP subunits takes place in peripheral punctate spots.

An interesting observation from the TLM experiments was that the majority of peripheral punctate spots and tubules stayed at a fixed position on the plasma membrane of the protoplast during the experiment, suggesting that they were somehow anchored. Since the cytoskeleton is known to function in the positioning and anchorage of organelles (Morris, 2003; Starr & Han, 2003; Takagi, 2003), we assessed whether microtubules or actin filaments were responsible for the anchorage of peripheral punctate spots and tubules. Therefore, protoplasts infected with CPMV MP–GFP were treated with inhibitors of microtubules and actin filaments (oryzalin and latrunculin B) as described previously (Pouwels *et al.*, 2002b), and at 42 h p.i., these protoplasts were embedded in 1·3 % LMP agarose containing the inhibitors. TLM experiments performed on these protoplasts at 46 h p.i. (data not shown) showed that disruption of the cytoskeleton did not mobilize the peripheral punctate spots and tubules and that therefore the cytoskeleton probably does not play a role in anchorage of foci at the plasma membrane. The fluorescent marker proteins GFP–MPD (the microtubule-binding domain of the microtubule-associated

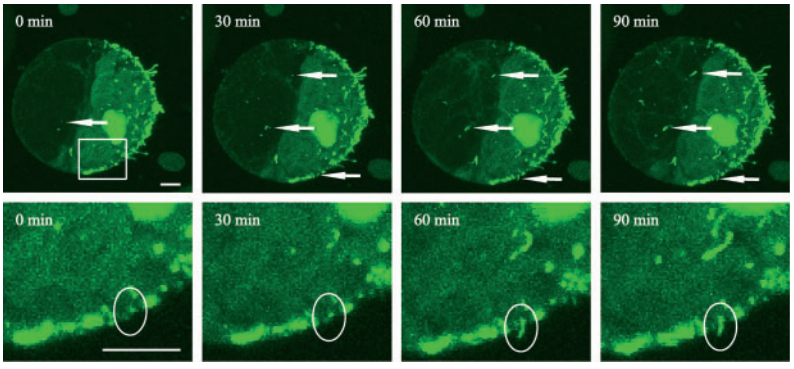

Fig. 1. Time-lapse microscopy of an embedded protoplast infected with CPMV MP–GFP. The upper panel shows the whole protoplast, while the lower panel focuses on the part indicated with the white rectangle in the first picture of the upper panel. Arrows indicate some peripheral punctate spots that were replaced with tubules. Images shown are confocal fluorescence micrographs of a projection of serial optical sections. Bars, 5 μm.

protein 4; Olson *et al.*, 1995) and YFP–talin (Pfaff *et al.*, 1998), labelling microtubules and actin filaments, respectively, were used to show that the inhibitors did indeed disrupt the cytoskeleton under these conditions (data not shown), as previously described (Pouwels *et al.*, 2002b).

MP molecules interact within the tubule

To confirm the notion that tubules are multimers of MP molecules, MP–MP interaction in tubules was determined by performing FRET experiments in living cells. Since CFP and YFP form a suitable donor/acceptor couple for FRET, fusions between MP and both CFP and YFP (MP–YFP and MP–CFP) were used to determine FRET in tubules. These proteins were transiently expressed in protoplasts after transfection with equal amounts of pMON-MP-YFP (Pouwels *et al.*, 2003) and pMON-MP-CFP, which contained the MP–YFP and MP–CFP coding regions under the control of a double 35S promoter. As expected, some of these protoplasts formed tubules that contained both MP–CFP and MP–YFP (Fig. 2a).

FRET was determined using APB (see Methods). Images obtained before and after bleaching (Fig. 2b) showed that CFP fluorescence increased after bleaching of YFP, indicating that FRET indeed occurred between MP–CFP and MP–YFP. To quantify the increase in CFP fluorescence, CFP fluorescence intensity was measured in the bleached area

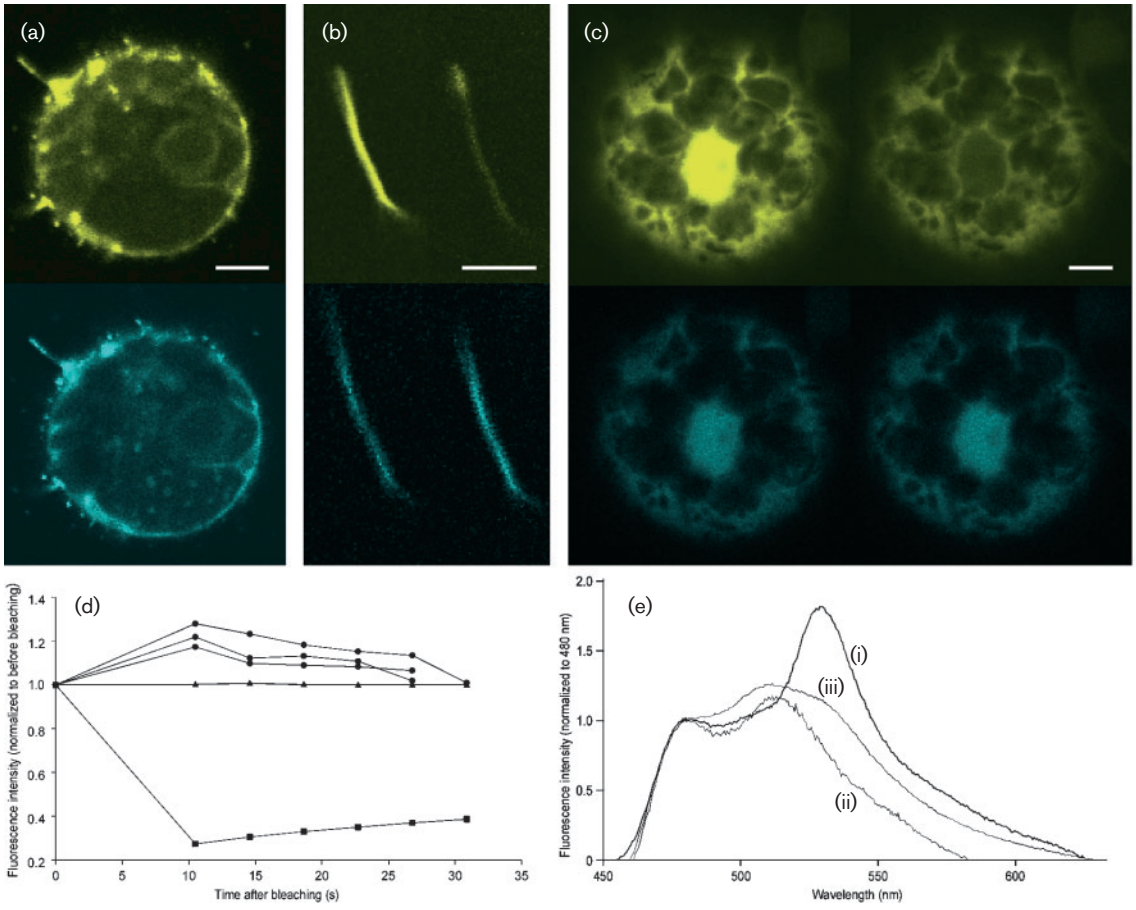

Fig. 2. Determination of FRET in protoplasts expressing MP–YFP and MP–CFP or free YFP and free CFP. (a)–(c) Confocal fluorescence micrographs of single optical sections. The upper panel shows the YFP signal and the lower panel the CFP signal. Bars, 5 μm. (a) Localization of transiently expressed MP–CFP and MP–YFP in protoplasts. (b, c) APB analysis of a tubule containing both MP–CFP and MP–YFP (b) or a nucleus containing both free CFP and free YFP (c). In (b) and (c), the pictures on the left show fluorescence before bleaching and the pictures on the right show fluorescence immediately after bleaching. (d) Examples of APB data obtained for tubules containing both MP–CFP and MP–YFP (● and ■) or a nucleus containing both free CFP and free YFP (▲). For comparison, the fluorescence intensities were normalized to the fluorescence intensities before bleaching. ●, MP–CFP fluorescence in three different tubules; ▲, CFP fluorescence in the nucleus; ■, MP–YFP fluorescence in a representative tubule. (e) FRET-SPIM emission spectra of a tubule containing both MP–CFP and MP–YFP (i), a tubule only containing MP–CFP (ii) or the cytoplasm of a cell containing both MP–CFP and MP–YFP (iii). For comparison, the emission spectra were normalized to the fluorescence intensity at 480 nm, one of the two emission peaks of CFP (ii).

(Fig. 2d), revealing that the mean increase in CFP fluorescence was 19·4 % ± 4·7 (± SEM; $n = 10$ tubules, each from a different cell). The relatively large variation in the increase in CFP fluorescence could partly be explained by the variation in YFP bleaching efficiencies and MP–CFP/MP–YFP expression ratios. From the increase in CFP fluorescence, the mean FRET efficiency and distance between YFP and CFP were calculated to be 16 % and 6·4 nm, respectively (Kenworthy, 2001). Since YFP fluorescence was not completely bleached (mean 65 %; Fig. 2d), the actual FRET efficiency will be higher and the actual distance between CFP and YFP will be lower. This distance between CFP and YFP conformed to the assumption that tubules are multimers of MP subunits, assuming that MP is a globular protein with a diameter of approximately 4 nm.

As a control, similar APB experiments were performed on protoplasts transfected with equal amounts of pMON-CFP and pMON-YFP, containing the CFP and YFP coding regions, respectively, under the control of a double 35S promoter. In these cells, the whole nucleus, where most of the CFP and YFP accumulates, was bleached, and images taken before and after bleaching (Fig. 2c) indicated that CFP fluorescence did not increase following bleaching of YFP. Quantification of CFP fluorescence intensity (Fig. 2d) confirmed that free CFP fluorescence did not increase after bleaching of free YFP, showing that FRET observed with MP–CFP and MP–YFP was specific.

To confirm FRET between MP–CFP and MP–YFP using an independent technique, FRET-SPIM experiments were performed (Fig. 2e) (Immink *et al.*, 2002). In these experiments, the emission spectra from tubules containing MP–CFP and MP–YFP, excited with light of 435 nm (which will only excite CFP), were recorded. The emission spectra showed that tubules containing MP–CFP and MP–YFP (Fig. 2e, curve i), but not tubules containing only MP–CFP (Fig. 2e, curve ii) or MP–YFP (data not shown) or cytoplasm containing both MP–CFP and MP–YFP (Fig. 2e, curve iii), showed a peak at 527 nm, characteristic of YFP emission. These spectra thus confirmed the occurrence of FRET between MP–CFP and MP–YFP in the tubule, showing interactions between MP molecules.

When the bleached area of the tubule, used to determine FRET, was monitored for several hours (data not shown), no fluorescence recovery was observed, showing that bleaching was irreversible and that MP–YFP was not able to diffuse within the tubule. Together with the observed FRET between MP–CFP and MP–YFP, this observation indicated that MP molecules within tubules interacted to form a highly organized multimer.

A direct interaction between the tubule and the surrounding plasma membrane does not occur

CPMV MP does not contain any of the plasma membrane interaction domains determined to date, although in plant tissue, tubules are almost exclusively formed at the plasma membrane (Kim & Fulton, 1971; van der Scheer & Groenewegen, 1971) and tubules on protoplasts are always tightly surrounded by the plasma membrane (van Lent *et al.*, 1991). Therefore, it was interesting to determine whether tubules, either directly or indirectly, interacted with the surrounding plasma membrane and, if so, how tight this interaction was. We hypothesized that if the interaction between the tubule and the plasma membrane was very tight, plasma membrane-associated proteins should be excluded from the plasma membrane surrounding the tubule due to lack of space. On the other hand, if the interaction was loose, plasma membrane-associated proteins should be able to get into and diffuse within the plasma membrane surrounding the tubule.

First, we tested whether plasma membrane-associated proteins were excluded from tubules. For this, YFP fused to the 40 C-terminal amino acids (the hypervariable region) of Rho of plant 7 from *Z. mays* (Zm7hvr) (Vermeer *et al.*, 2004), which contains a myristylation site, was used as a marker protein. As expected (Vermeer *et al.*, 2004), protoplasts transfected with pMON-YFP-Zm7hvr, which contains the YFP–Zm7hvr coding region under the control of a double 35S promoter, showed fluorescence mainly in the plasma membrane (Fig. 3a). In protoplasts with a very high expression level, some YFP–Zm7hvr was also observed in the cytoplasm, most likely due to saturation of the plasma membrane. When protoplasts were inoculated with pMON-YFP-Zm7hvr and CPMV, YFP–Zm7hvr also accumulated in tubules (Fig. 3b, arrows), indicating that this small plasma membrane-associated protein (YFP–Zm7hvr, 27 kDa, a cylinder with a diameter of 3 nm and a length of 4 nm) was not excluded from the plasma membrane around tubules. It was not known whether YFP–Zm7hvr (or 110–YFP–Zm7hvr, see below) accumulated to the same extent in the plasma membrane surrounding the tubule as in the plasma membrane outside the tubule, since we were not able to determine the fluorescence densities accurately in these regions.

To determine whether larger proteins could also be accommodated in the plasma membrane around tubules, a construct encoding a fusion between YFP–Zm7hvr and the 110 kDa protein, encoded by CPMV RNA1 (Pouwels *et al.*, 2002a), was used (pMON-110-YFP–Zm7hvr). Protoplasts inoculated with pMON-110-YFP-Zm7hvr revealed that 110–YFP–Zm7hvr also accumulated in the plasma membrane (Fig. 3c). Previous studies have shown that the 110 kDa protein is stable in protoplasts (van Bokhoven *et al.*, 1993) and data presented below indicated that 110–YFP–Zm7hvr was also a stable protein. Protoplasts inoculated with pMON-110-YFP-Zm7hvr and CPMV showed accumulation of 110–YFP–Zm7hvr in tubules (Fig. 3d, arrows), indicating that rather large proteins (approx. 140 kDa, with an estimated diameter of 7 nm) could also be accommodated in the plasma membrane around the tubule. These data on the presence of plasma membrane-bound proteins in tubules indicated that the

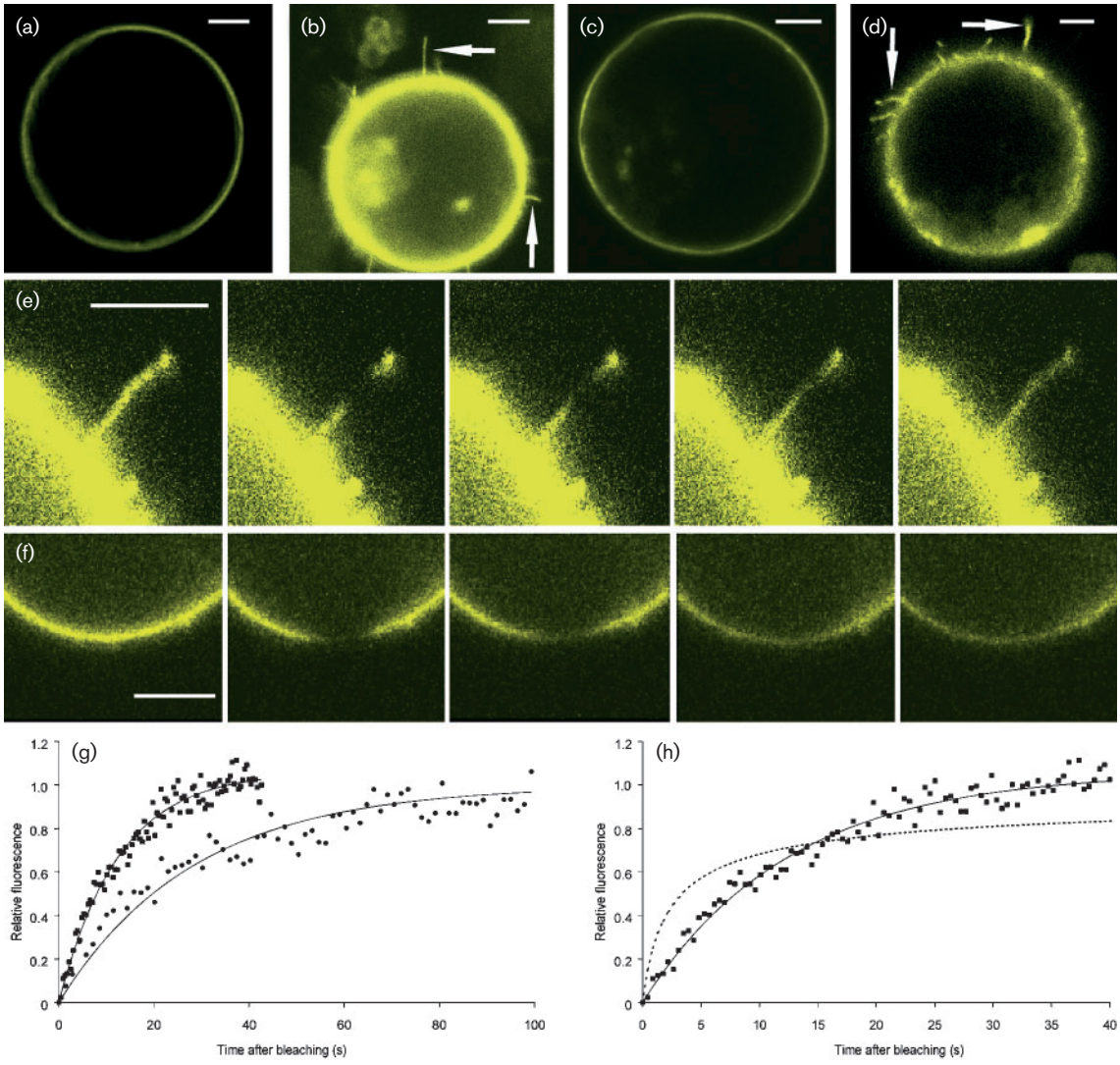

Fig. 3. FRAP analysis of YFP–Zm7hvr and 110–YFP–Zm7hvr in the plasma membrane surrounding the tubule and outside the tubule. (a, b) Localization of YFP–Zm7hvr in non-infected cowpea protoplasts (a) and cowpea protoplasts infected with CPMV (b). (c, d) Localization of 110–YFP–Zm7hvr in non-infected cowpea protoplasts (c) and cowpea protoplasts infected with CPMV (d). (e, f) Monitoring of fluorescence recovery of 110–YFP–Zm7hvr in the plasma membrane surrounding the tubule (e) and the plasma membrane outside tubules (f). The pictures in (e) and (f) were taken before bleaching and approximately 0, 6, 20 and 100 s after bleaching (left to right). (g) Normalized FRAP data (FN_0 was set to 0 and FN_∞ to 1; see Methods) recorded for YFP–Zm7hvr (■) and 110–YFP–Zm7hvr (●) in the plasma membrane surrounding the tubule. Lines represent the theoretical recovery curves after fitting the data to equation 1. (h) Normalized FRAP data recorded for YFP–Zm7hvr (■) in the plasma membrane surrounding the tubule (same data as shown in Fig. 3g). The solid line represents the theoretical recovery curve after fitting to equation 1 and the dotted line represents the theoretical recovery curve after fitting to the standard recovery curve for one-dimensional diffusion (Ellenberg *et al.*, 1997). Images shown in (a–f) are confocal fluorescence micrographs of single optical sections. Bars, 5 μm.

interaction between the plasma membrane and the tubule, if any, is not very tight and that therefore tubules do not interact directly with the plasma membrane.

Another parameter that could give insight into the tightness of the interaction between tubules and the plasma membrane is the diffusion coefficients of YFP–Zm7hvr and 110–YFP–Zm7hvr. These diffusion coefficients were determined in the membrane surrounding the tubule and the plasma membrane outside the tubule using FRAP (see Methods). Surprisingly, the mobile fraction (i.e. the fraction of bleached fluorescent protein that is replaced with non-bleached fluorescent protein during the FRAP experiment) of both YFP–Zm7hvr and 110–YFP–Zm7hvr was rather small (30–50 %; Fig. 3e and f) compared with integral plasma membrane proteins, which were all studied in

animal cells (> 90 %; Adams *et al.*, 1998; Haggie *et al.*, 2003; Umenishi *et al.*, 2000). The mobile fraction was comparable in both the plasma membrane surrounding the tubule and the plasma membrane outside the tubule, showing that the small mobile fractions were due to an intrinsic property of the plasma membrane interaction domain and not due to the presence of the tubule. Currently, we cannot explain why YFP–Zm7hvr and 110–YFP–Zm7hvr had such relatively small mobile fractions. In spite of their small mobile fractions, YFP–Zm7hvr and 110–YFP–Zm7hvr could be used in this experiment, since calculation of the diffusion coefficient of a mobile fraction is independent of the size of this fraction (see Methods), and the diffusion coefficients of YFP–Zm7hvr and 110–YFP–Zm7hvr in the plasma membrane outside the tubules (Table 1) were comparable to those of other plasma membrane-associated proteins (Adams *et al.*, 1998; Haggie *et al.*, 2003; Jans *et al.*, 1990; Meissner & Haberlein, 2003; Tardin *et al.*, 2003; Umenishi *et al.*, 2000).

The diffusion coefficients were determined by bleaching YFP, monitoring the fluorescence recovery in time (Fig. 3e and f show 110–YFP–Zm7hvr) and fitting the fluorescence recovery to the standard recovery curve for two-dimensional diffusion in a uniform circle (equation 1; Fig. 3g shows YFP–Zm7hvr and 110–YFP–Zm7hvr in the plasma membrane surrounding the tubule). On theoretical grounds, the standard recovery curve for one-dimensional diffusion (Ellenberg *et al.*, 1997) should be used for calculation of the diffusion coefficients in the plasma membrane surrounding the tubule. The fluorescence recoveries we observed, however, fitted much better to the standard recovery curve for two-dimensional diffusion (Fig. 3h) and therefore this curve was used to calculate diffusion coefficients (Table 1, see Methods). These data showed that in the plasma membrane surrounding the tubule, diffusion of both YFP–Zm7hvr and 110–YFP–Zm7hvr was significantly slower ($P \leqslant 0{\cdot}001$, Wilcoxon test) than in the plasma membrane outside the tubule, implicating that diffusion of these plasma membrane-associated proteins was hindered by the presence of the tubule. Furthermore, the diffusion coefficient of 110–YFP–Zm7hvr in the plasma membrane surrounding the tubule was significantly lower than that of YFP–Zm7hvr ($P < 0{\cdot}005$), while, as expected, the diffusion coefficients of YFP–Zm7hvr and 110–YFP–Zm7hvr in the plasma membrane outside tubular structures were not significantly different ($P \leqslant 0{\cdot}19$). Together these data indicated an interaction between the tubule and the surrounding plasma membrane. Since the tubule probably does not interact directly with the plasma membrane, as suggested by the presence of YFP–Zm7hvr and 110–YFP–Zm7hvr in the plasma membrane surrounding the tubule (see above), this interaction will be indirect, presumably through a host plasma membrane protein.

Table 1. Diffusion coefficients of YFP–Zm7hvr and 110–YFP–Zm7hvr in the plasma membrane surrounding the tubule and outside the tubule, as determined using FRAP

All values in are given as mean ± SEM ($\mu m^2\ s^{-1}$). The number (n) of analysed samples is shown in parentheses.

Plasmid	Around tubule (n)	Outside tubule (n)
YFP–Zm7hvr	0·047 ± 0·006 (18)	0·090 ± 0·007 (27)
110–YFP–Zm7hvr	0·007 ± 0·001 (9)	0·119 ± 0·018 (16)

DISCUSSION

In protoplasts, CPMV MP is transported to the plasma membrane where it quickly accumulates in peripheral punctate spots and tubules (Gopinath *et al.*, 2003; Pouwels *et al.*, 2002b, 2003). Using TLM and FRAP, we have shown that peripheral punctate spots are dynamic structures, which constantly exchange MP–GFP subunits. Some of the peripheral punctate spots could grow out to become a tubule, indicating that these spots act as precursors of tubules, as suggested previously (Huang *et al.*, 2000; Pouwels *et al.*, 2002b). Possibly, peripheral punctate spots simply represent MP accumulations, which, by incorporation of new subunits, grow out to become a tubule. It is unlikely that all peripheral punctate spots are short tubules, since most spots did not grow out to become a tubule, although they were able to incorporate new MP–GFP subunits. Alternatively, only a subset of the peripheral punctate spots may attain the proper conformation for tubule formation. The observation that peripheral punctate spots that grow out into a tubule are generally small suggested that large peripheral punctate spots might have lost the ability to become a tubule or that these spots are artefacts of the protoplast system.

The observation that most of the peripheral punctate spots were immobile suggested that these spots are somehow anchored to the plasma membrane. Based on inhibitor studies, the cytoskeleton did not seem to play a role in this anchoring. The co-localization of the peripheral punctate spots of *Tobacco mosaic virus* MP with the peripheral endoplasmic reticulum (ER) (Heinlein *et al.*, 1998) suggests that association with the ER could be responsible for the immobility of peripheral punctate spots. The extensive movement of peripheral ER strands in time (data not shown), however, seemed to indicate that the peripheral ER was not responsible for the anchoring of peripheral punctate spots made by CPMV MP. Alternatively, the peripheral punctate spots observed using CLSM may simply be too big to move, since probably more than 100 MP–GFP subunits are part of these spots (Dundr *et al.*, 2002).

Using two independent techniques (APB and FRET-SPIM), the occurrence of FRET between MP–CFP and MP–YFP was demonstrated in the tubule, showing that MP subunits interacted within the tubule. Furthermore, the observation that MP–YFP was immobile within tubules suggested that tubules consisted of a stable MP multimer. Previously, interaction between MP subunits has been shown to occur *in vitro* using a blot overlay assay (Carvalho *et al.*, 2003), and

co-transfection experiments with wt and mutant MPs have indicated that interaction between MP subunits is required for targeting of MP to the cell periphery (Pouwels *et al.*, 2003).

Although CPMV MP does not contain any of the currently known membrane-association domains, previous observations have suggested an interaction of the tubule with the plasma membrane (Kim & Fulton, 1971; van der Scheer & Groenewegen, 1971; van Lent *et al.*, 1991). Accumulation of plasma membrane-bound proteins (YFP–Zm7hvr and 110–YFP–Zm7hvr) in the plasma membrane surrounding the tubule indicated that MP subunits in tubules made on protoplasts did not interact directly with the surrounding plasma membrane. To gain more insight into the putative interactions between tubules and the plasma membrane, the diffusion coefficients of YFP–Zm7hvr and 110–YFP–Zm7hvr in the plasma membrane surrounding the tubule and the plasma membrane outside the tubule were determined using FRAP. For calculation of the diffusion coefficients from the FRAP data, the standard recovery curve for two-dimensional diffusion in a uniform circle (equation 1; Axelrod *et al.*, 1976) was used, although on theoretical grounds one might expect that for calculation of the diffusion coefficients in the plasma membrane surrounding the tubule, the standard recovery curve for one-dimensional diffusion (Ellenberg *et al.*, 1997) should be used. However, the fluorescence recovery we observed in the plasma membrane surrounding the tubules fitted much better to the standard recovery curve for two-dimensional diffusion than to that for one-dimensional diffusion (Fig. 3h).

Irrespective of the formula used to calculate the diffusion coefficient, the FRAP experiments revealed that plasma membrane-associated proteins accumulated and diffused in the plasma membrane surrounding the tubule, supporting the notion that the interaction between the tubule and the surrounding plasma membrane is not very tight. However, in the plasma membrane surrounding the tubule, diffusion of 110–YFP–Zm7hvr was clearly slower than diffusion of YFP–Zm7hvr (Fig. 3g; Table 1), indicating that an indirect interaction between the tubule and the surrounding plasma membrane had taken place. This indirect interaction probably occurs via a host protein in the plasma membrane, which would leave enough space for plasma membrane-associated proteins to be inserted, but too little space for them to diffuse freely. Since tubules are also formed on protoplasts of non-host plants (Wellink *et al.*, 1993) and on insect cells (Kasteel *et al.*, 1996), this host factor is probably conserved among plant and animal species. An alternative explanation is that a direct interaction does occur between the tubule and the surrounding plasma membrane, which is transient and can temporarily be disrupted by plasma membrane-associated molecules like YFP–Zm7hvr and 110–YFP–Zm7hvr.

The (indirect) interaction between the tubule and the plasma membrane was further supported by the observation that diffusion of both YFP–Zm7hvr and 110–YFP–Zm7hvr was hindered in the tubule, as shown by lower diffusion rates in the plasma membrane surrounding the tubule than in the plasma membrane outside tubules. This difference, however, might be smaller than described in Table 1, since using the standard recovery curve for two-dimensional diffusion to calculate the diffusion coefficients in the plasma membrane surrounding the tubule may lead to an underestimation of these diffusion coefficients. Furthermore, an overestimation of the diffusion coefficient in the plasma membrane outside tubules due to constant exchange of YFP–Zm7hvr or 110–YFP–Zm7hvr between the plasma membrane and the cytoplasm cannot be excluded.

Due to technical limitations, the studies described in this paper were carried out in a protoplast expression system and we have not been able to extend these studies to infected plant tissue. Since tubules in plant tissue and on protoplasts are morphologically very similar (van Lent *et al.*, 1991) and the behaviour of mutant MPs is comparable in plant tissue and protoplasts (Gopinath *et al.*, 2003; Pouwels *et al.*, 2003), it is highly unlikely that tubules assemble differently in protoplasts and infected leaf cells. However, we cannot rule out the possibility that the interaction of the tubule with the surrounding plasma membrane (through a host protein) is stronger in infected plant tissue.

ACKNOWLEDGEMENTS

The authors wish to thank Gerard van der Krogt for providing pMON-ECFP and Frans Leermakers and Renko de Vries from the Laboratory of Physical Chemistry and Colloid Science of Wageningen University for fruitful discussions. Furthermore, Mark Hink from the MicroSpectroscopy Centre is acknowledged for critically reading the manuscript.

REFERENCES

Adams, C. L., Chen, Y. T., Smith, S. J. & Nelson, W. J. (1998). Mechanisms of epithelial cell–cell adhesion and cell compaction revealed by high-resolution tracking of E-cadherin-green fluorescent protein. *J Cell Biol* **142**, 1105–1119.

Axelrod, D., Koppel, D. E., Schlessinger, J., Elson, E. & Webb, W. W. (1976). Mobility measurement by analysis of fluorescence photobleaching recovery kinetics. *Biophys J* **16**, 1055–1069.

Bastiaens, P. I. & Jovin, T. M. (1996). Microspectroscopic imaging tracks the intracellular processing of a signal transduction protein: fluorescent-labeled protein kinase C beta I. *Proc Natl Acad Sci U S A* **93**, 8407–8412.

Bastiaens, P. I., Majoul, I. V., Verveer, P. J., Soling, H. D. & Jovin, T. M. (1996). Imaging the intracellular trafficking and state of the AB5 quaternary structure of cholera toxin. *EMBO J* **15**, 4246–4253.

Bertens, P., Wellink, J., Goldbach, R. & van Kammen, A. (2000). Mutational analysis of the cowpea mosaic virus movement protein. *Virology* **267**, 199–208.

Bertens, P., Heijne, W., van der Wel, N., Wellink, J. & van Kammen, A. (2003). Studies on the C-terminus of the cowpea mosaic virus movement protein. *Arch Virol* **148**, 265–279.

Canto, T. & Palukaitis, P. (1999). Are tubules generated by the 3a protein necessary for cucumber mosaic virus movement? *Mol Plant Microbe Interact* **12**, 985–993.

Carvalho, C. M., Wellink, J., Ribeiro, S. G. W. G. R. & van Lent, J. W. M. (2003). The C-terminal region of the movement protein of cowpea mosaic virus is involved in binding to the large but not to the small coat protein. *J Gen Virol* **84**, 2271–2277.

Dundr, M., McNally, J. G., Cohen, J. & Misteli, T. (2002). Quantitation of GFP-fusion proteins in single living cells. *J Struct Biol* **140**, 92–99.

Eggen, R., Verver, J., Wellink, J., Pleij, K., van Kammen, A. & Goldbach, R. (1989). Analysis of sequences involved in cowpea mosaic virus RNA replication using site-specific mutants. *Virology* **173**, 456–464.

Ellenberg, J., Siggia, E. D., Moreira, J. E., Smith, C. L., Presley, J. F., Worman, H. J. & Lippincott-Schwartz, J. (1997). Nuclear membrane dynamics and reassembly in living cells: targeting of an inner nuclear membrane protein in interphase and mitosis. *J Cell Biol* **138**, 1193–1206.

Gerlich, D. & Ellenberg, J. (2003). 4D imaging to assay complex dynamics in live specimens. *Nat Cell Biol* **5**, S14–S19.

Gopinath, K., Wellink, J., Porta, C., Taylor, K. M., Lomonossoff, G. P. & van Kammen, A. (2000). Engineering cowpea mosaic virus RNA-2 into a vector to express heterologous proteins in plants. *Virology* **267**, 159–173.

Gopinath, K., Bertens, P., Pouwels, J., Marks, H., van Lent, J., Wellink, J. & van Kammen, A. (2003). Intracellular distribution of cowpea mosaic virus movement protein as visualised by green fluorescent protein fusions. *Arch Virol* **148**, 2099–2114.

Haggie, P. M., Stanton, B. A. & Verkman, A. S. (2003). Increased diffusional mobility of CFTR at the plasma membrane after deletion of its C-terminus PDZ-binding motif. *J Biol Chem* **279**, 5494–5500.

Haywood, V., Kragler, F. & Lucas, W. J. (2002). Plasmodesmata: pathways for protein and ribonucleoprotein signaling. *Plant Cell* **14**, S303–S325.

Heinlein, M., Padgett, H. S., Gens, J. S., Pickard, B. G., Casper, S. J., Epel, B. L. & Beachy, R. N. (1998). Changing patterns of localization of the tobacco mosaic virus movement protein and replicase to the endoplasmic reticulum and microtubules during infection. *Plant Cell* **10**, 1107–1120.

Huang, Z., Han, Y. & Howell, S. H. (2000). Formation of surface tubules and fluorescent foci in *Arabidopsis thaliana* protoplasts expressing a fusion between the green fluorescent protein and the cauliflower mosaic virus movement protein. *Virology* **271**, 58–64.

Immink, R. G., Gadella, T. W., Jr, Ferrario, S., Busscher, M. & Angenent, G. C. (2002). Analysis of MADS box protein–protein interactions in living plant cells. *Proc Natl Acad Sci U S A* **99**, 2416–2421.

Jans, D. A., Peters, R. & Fahrenholz, F. (1990). Lateral mobility of the phospholipase C-activating vasopressin V1-type receptor in A7r5 smooth muscle cells: a comparison with the adenylate cyclase-coupled V2-receptor. *EMBO J* **9**, 2693–2699.

Karpova, T. S., Baumann, C. T., He, L., Wu, X., Grammer, A., Lipsky, P., Hager, G. L. & McNally, J. G. (2003). Fluorescence resonance energy transfer from cyan to yellow fluorescent protein detected by acceptor photobleaching using confocal microscopy and a single laser. *J Microsc* **209**, 56–70.

Kasteel, D., Wellink, J., Verver, J., van Lent, J., Goldbach, R. & van Kammen, A. (1993). The involvement of cowpea mosaic virus M RNA-encoded proteins in tubule formation. *J Gen Virol* **74**, 1721–1724.

Kasteel, D. T., Perbal, M. C., Boyer, J. C., Wellink, J., Goldbach, R. W., Maule, A. J. & van Lent, J. W. (1996). The movement proteins of cowpea mosaic virus and cauliflower mosaic virus induce tubular structures in plant and insect cells. *J Gen Virol* **77**, 2857–2864.

Kasteel, D. T., Wellink, J., Goldbach, R. W. & van Lent, J. W. (1997). Isolation and characterization of tubular structures of cowpea mosaic virus. *J Gen Virol* **78**, 3167–3170.

Kenworthy, A. K. (2001). Imaging protein–protein interactions using fluorescence resonance energy transfer microscopy. *Methods* **24**, 289–296.

Kim, K. S. & Fulton, J. P. (1971). Tubules with viruslike particles in leaf cells infected with bean pod mottle virus. *Virology* **43**, 329–337.

Lazarowitz, S. G. & Beachy, R. N. (1999). Viral movement proteins as probes for intracellular and intercellular trafficking in plants. *Plant Cell* **11**, 535–548.

Mas, P. & Beachy, R. N. (1998). Distribution of TMV movement protein in single living protoplasts immobilized in agarose. *Plant J* **15**, 835–842.

Meissner, O. & Haberlein, H. (2003). Lateral mobility and specific binding to $GABA_A$ receptors on hippocampal neurons monitored by fluorescence correlation spectroscopy. *Biochemistry* **42**, 1667–1672.

Morris, N. R. (2003). Nuclear positioning: the means is at the ends. *Curr Opin Cell Biol* **15**, 54–59.

Olson, K. R., McIntosh, J. R. & Olmsted, J. B. (1995). Analysis of MAP 4 function in living cells using green fluorescent protein (GFP) chimeras. *J Cell Biol* **130**, 639–650.

Pfaff, M., Liu, S., Erle, D. J. & Ginsberg, M. H. (1998). Integrin β cytoplasmic domains differentially bind to cytoskeletal proteins. *J Biol Chem* **273**, 6104–6109.

Phair, R. D. & Misteli, T. (2001). Kinetic modelling approaches to *in vivo* imaging. *Nat Rev Mol Cell Biol* **2**, 898–907.

Pouwels, J., Carette, J. E., Van Lent, J. & Wellink, J. (2002a). Cowpea mosaic virus: effects on host cell processes. *Mol Plant Pathol* **3**, 411–418.

Pouwels, J., van Der Krogt, G. N., van Lent, J., Bisseling, T. & Wellink, J. (2002b). The cytoskeleton and the secretory pathway are not involved in targeting the cowpea mosaic virus movement protein to the cell periphery. *Virology* **297**, 48–56.

Pouwels, J., Kornet, N., van Bers, N., Guighelaar, T., van Lent, J., Bisseling, T. & Wellink, J. (2003). Identification of distinct steps during tubule formation by the movement protein of cowpea mosaic virus. *J Gen Virol* **84**, 3485–3494.

Salmon, E. D., Leslie, R. J., Saxton, W. M., Karow, M. L. & McIntosh, J. R. (1984). Spindle microtubule dynamics in sea urchin embryos: analysis using a fluorescein-labeled tubulin and measurements of fluorescence redistribution after laser photobleaching. *J Cell Biol* **99**, 2165–2174.

Satoh, H., Matsuda, H., Kawamura, T., Isogai, M., Yoshikawa, N. & Takahashi, T. (2000). Intracellular distribution, cell-to-cell trafficking and tubule-inducing activity of the 50 kDa movement protein of apple chlorotic leaf spot virus fused to green fluorescent protein. *J Gen Virol* **81**, 2085–2093.

Sekar, R. B. & Periasamy, A. (2003). Fluorescence resonance energy transfer (FRET) microscopy imaging of live cell protein localizations. *J Cell Biol* **160**, 629–633.

Shah, K., Russinova, E., Gadella, T. W., Jr, Willemse, J. & De Vries, S. C. (2002). The *Arabidopsis* kinase-associated protein phosphatase controls internalization of the somatic embryogenesis receptor kinase 1. *Genes Dev* **16**, 1707–1720.

Starr, D. A. & Han, M. (2003). ANChors away: an actin based mechanism of nuclear positioning. *J Cell Sci* **116**, 211–216.

Takagi, S. (2003). Actin-based photo-orientation movement of chloroplasts in plant cells. *J Exp Biol* **206**, 1963–1969.

Tardin, C., Cognet, L., Bats, C., Lounis, B. & Choquet, D. (2003). Direct imaging of lateral movements of AMPA receptors inside synapses. *EMBO J* **22**, 4656–4665.

Umenishi, F., Verbavatz, J. M. & Verkman, A. S. (2000). cAMP regulated membrane diffusion of a green fluorescent protein–aquaporin 2 chimera. *Biophys J* **78**, 1024–1035.

van Bokhoven, H., Verver, J., Wellink, J. & van Kammen, A. (1993). Protoplasts transiently expressing the 200K coding sequence of cowpea mosaic virus B-RNA support replication of M-RNA. *J Gen Virol* **74**, 2233–2241.

van der Scheer, C. & Groenewegen, J. (1971). Structure in cells of *Vigna unguiculata* infected with cowpea mosaic virus. *Virology* **46**, 493–497.

van Lent, J. W., Wellink, J. & Goldbach, R. W. (1990). Evidence for the involvement of the 58K and 48K proteins in the intracellular movement of cowpea mosaic virus. *J Gen Virol* **71**, 219–223.

van Lent, J., Storms, M., van der Meer, F., Wellink, J. & Goldbach, R. (1991). Tubular structures involved in movement of cowpea mosaic virus are also formed in infected cowpea protoplasts. *J Gen Virol* **72**, 2615–2623.

Vermeer, J. E., van Munster, E. B., Vischer, N. O. & Gadella, T. W., Jr (2004). Probing plasma membrane microdomains in cowpea protoplasts using lipidated GFP-fusion proteins and multimode FRET microscopy. *J Microsc* **214**, 190–200.

Wellink, J., van Lent, J. W., Verver, J., Sijen, T., Goldbach, R. W. & van Kammen, A. (1993). The cowpea mosaic virus M RNA-encoded 48-kilodalton protein is responsible for induction of tubular structures in protoplasts. *J Virol* **67**, 3660–3664.

Wouters, F. S., Bastiaens, P. I., Wirtz, K. W. & Jovin, T. M. (1998). FRET microscopy demonstrates molecular association of non-specific lipid transfer protein (nsL-TP) with fatty acid oxidation enzymes in peroxisomes. *EMBO J* **17**, 7179–7189.